HIGH PERFORMANCE POLYSILICON NEMS FABRICATED AT LOW TEMPERATURE WITH UV LASER ANNEALING

*Issam Ouerghi, Marc Sansa, Laurent Duraffourg, Kevin Benedetto, Paul Besombes, *Karim Huet, *Fulvio Mazzamuto, *Ines Toque-Tresonne, Carine Ladner, Sebastien Kerdiles, Willy Ludurczak, and Thomas Ernst*
CEA, LETI, MINATEC Campus, 17 rue des Martyrs - 38054 GRENOBLE Cedex 9, France
*SCREEN LASSE, 14 rue Alexandre 92230 GENNEVILLIERS, France

ABSTRACT

In this paper, we present for the first time poly-Silicon nanowire (poly-Si NW) based NEMS resonators fabricated at very low temperature (300°C max) and recrystallized with a 308nm excimer laser for low cost co-integrated mass sensors on CMOS. Poly-Si NEMS performances have been systematically compared to crystalline silicon (c-Si) NEMS and most important resonator's figure of merit have been extracted. Within an excellent fabrication yield, the stability measurements of poly-Si NEMS lead to a mass resolution detection in air down to 190 zg ($\times 10^{-21}$g).

INTRODUCTION

The transition from MEMS to NEMS allows to drastically increase sensitivity and resolution of mass sensors and the NEMS-CMOS co-integration is essential to improve the efficiency of the electrical detection of the NEMS motion [1]. Nowadays only few groups work on this topic, as reported on the Table 1. The 3D fabrication of the NEMS after the back-end is the most cost effective and compact solution for the embedded sensors [6]. To protect the back-end interconnections, Poly-Si can be processed at low temperature and seems to be an excellent candidate to replace c-Si. UV laser is a promising solution to locally anneal, crystallize and activate dopants of a deposited amorphous layer. In this work, we have fabricated poly-Si NEMS at low temperature thanks to a room temperature a-Si deposition (sputtering) plus a XeCl excimer laser annealing.

FABRICATION

First, morphological and electrical study of the poly-Si properties according to the laser conditions has been performed. Figure 1 shows the sheet resistance as a function of the fluence. The resistance decreases with the fluence (explosive crystallization) until a threshold called super lateral growth crystallization (SLG) [7]. We selected two annealing conditions near the SLG regime to fabricate poly-Si NEMS, at 700 and 725mJ/cm² called polyA and polyB respectively with two dopant concentrations. XRD measurements have been performed in order to extract preferential orientations and grain sizes. However, no preferential orientation was found for every samples. As shown in Figure 2, the average grain sizes are between 30-50 nm depending on the grain orientation. It is probably due to the intra grain defects and also the high presence of argon in RT PVD silicon. No particular texture was observed, samples being randomly oriented. SIMS profiles after laser treatment show a uniform distribution of dopant atoms, highlighted in the figure 3. c-Si NEMS have been fabricated from a SOI wafer. Figure 4 and Figure 5 show

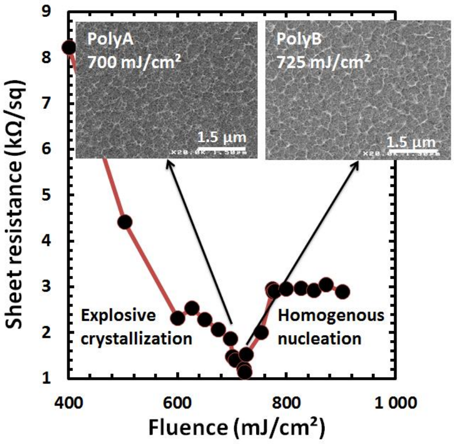

Figure 1: Poly-Si sheet resistance after laser annealing as a function of the fluence. Two laser conditions have been selected (700 and 725 mJ/cm²) for the NEMS fabrication. The top view SEM images illustrate the corresponding morphology.

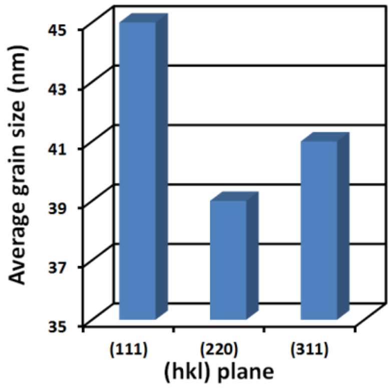

Figure 2: Average grain sizes of a polysilicon layer after laser annealing extracted with XRD measurement.

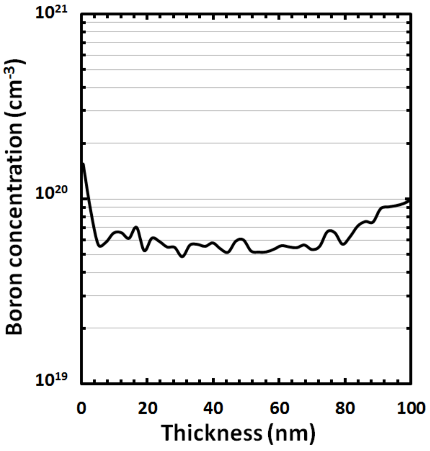

Figure 3: SIMS profile of boron concentration in a 100 nm poly-Si layer on oxide after laser annealing.

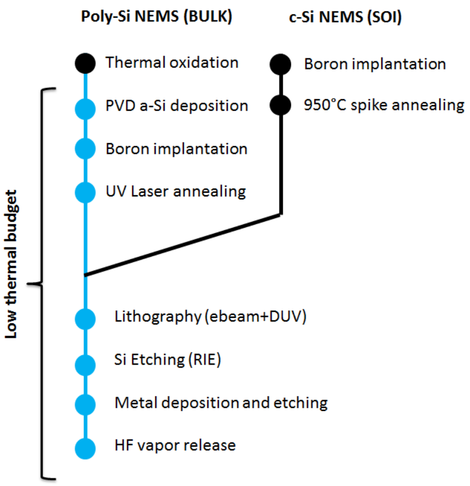

Figure 4: NEMS fabrication sequences for poly-Si and c-Si NEMS.

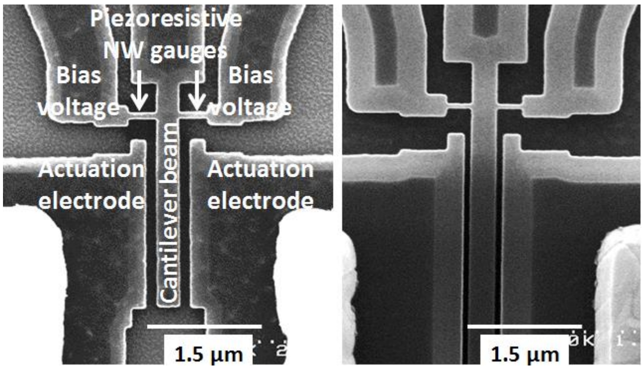

Figure 5: SEM micrograph of a (a) poly-Si NEMS and (b) c-Si NEMS. Characterized NEMS beam has a length of 3.2 µm and a width of 300 nm. Gauges have a length of 400 nm and a width of 80 nm.

c-Si and poly-Si NEMS process flows and photos respectively.

NEMS CHARACTERIZATION

The NEMS resonators consist in a cantilever with two nano-gauges for piezoresistive detection [8]. We performed a resonance analysis of the samples in air by measuring the electromechanical response at high frequency (HF) of every device in an open loop scheme with a downmixing method [9] as shown in Figure 6. Equivalent Signal to Background Ratio (SBR) of about 20-30 dB were found for every NEMS, and a Q factor of about 100. We also measured the stability frequency as shown in Figure 7 with the Allan deviation as a function of the integration time. We focused on an integration time of about 100ms, an appropriate value for gas sensing applications. As we can see, the higher the dopant concentration, the better the stability for both polyA and polyB. Knowing the resonator effective mass M_{eff}, the mass resolution can be extracted: $\delta m=\delta f/f\times 2M_{eff}$. The NEMS frequency stability has been measured for the entire wafers and the probability density function (PDF) of this parameter is represented in Figure 8 for the best splits. By Fitting a Gaussian distribution of the PDF, equivalent FWHM was found for poly-Si and c-Si NEMS at 3×10^{20} cm^{-3}. We can conclude that such a small average grain size

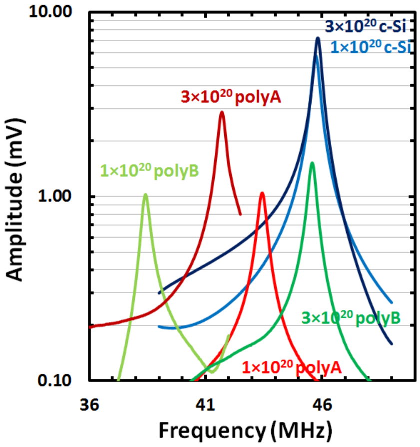

Figure 6: Resonance peak in air for different poly-Si and c-Si NEMS. SBR and Q factors are equivalent.

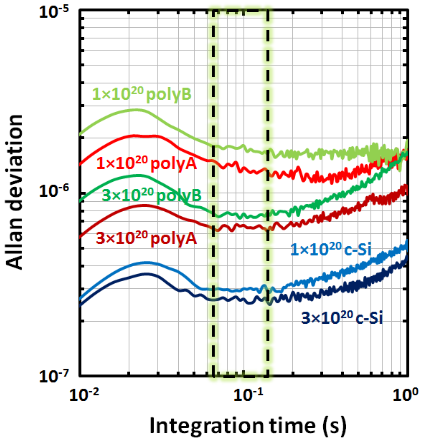

Figure 7: Allan deviation in air as a function of the integration time for different poly-Si and c-Si NEMS. The dashed window at about 100ms is the area of interest for the mass sensing application. Higher the dopant concentration, better the resonator stability.

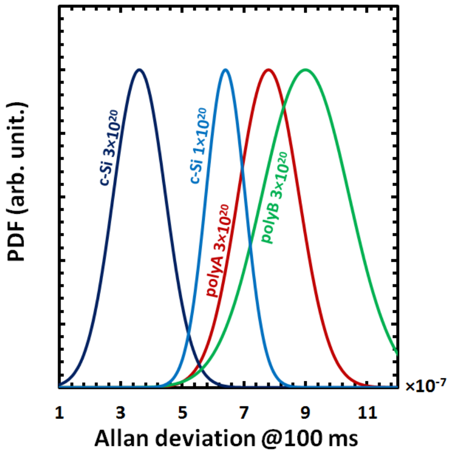

Figure 8: Probability density function as a function of Allan deviation for polyA, polyB at 3×10^{20} cm^{-3} and c-Si at different dopant concentrations. PolyA NEMS show a distribution of the stability comparable to c-Si.

coupled with a random structure enable to obtain a very low variability of NEMS properties. The best results were found with PolyA at 3×10^{20} cm^{-3} with a ratio of 94% functional NEMS. We also performed measurements in vacuum. Figure 9 shows the voltage noise at resonance of polyA without actuation. In this way, the thermomechanical noise and dynamic range (DR) can be extracted. All the results corresponding to polyA and c-Si NEMS 3×10^{20} cm^{-3} are summarized in Table 2.

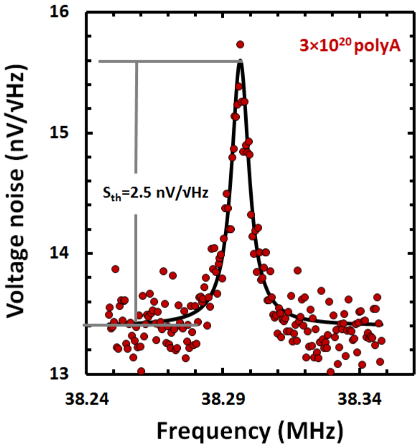

Figure 9: Vacuum resonance peak of polyA NEMS without actuation voltage allowing the thermomechanical noise extraction.

CONCLUSION

Poly-Si NEMS fabricated at very low temperature, show competitive performances compared to c-Si NEMS. The process is completely compatible with a CMOS back-end with a room temperature silicon deposition combined to UV laser annealing. For polyA, we found an average Allan deviation at 100ms in air as low as 8×10^{-7} providing a theoretical mass resolution at the zeptogram scale and an excellent yield (94%) paving the way for performant large scale NEMS array manufacturing.

Table 1. Recent monolithic NEMS-CMOS co-integrations benchmarking.

Device	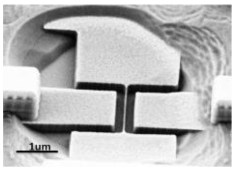	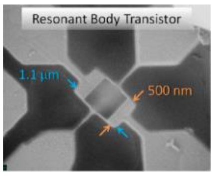	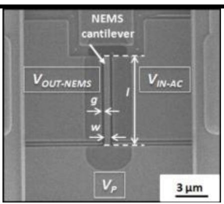	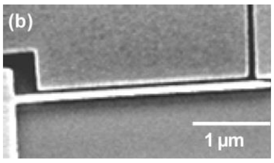
Actuation/detection	Capacitive/ Capacitive	Electrostatic/ Piezoresistive	Capacitive/ Capacitive	Switch
Materials	Poly-Si	Silicon	Silicon	Platinum
Critical dimension (nm)	60	220	160	60
Ref.	[2]	[3]	[4]	[5]

Table 2. Summary of the different extracted figures of merit for PolyA and c-Si NEMS. Knowing the effective sensor mass (M_{eff}=120 fg) and the frequency stability, the minimum mass resolution Δm can be calculated ($\Delta f/f=\Delta m/2M_{eff}$). Sfloor represent the noise plateau in Figure 9, S_j the Johnson noise and S_{th} the thermomechanical noise.

NEMS	***Q air/vacuum***	**Allan Dev. @100ms (x10^{-7})**	**Mass resolution (zg)**	**Yield (%)**	**S_{floor} (nV/√Hz)**	**S_j (nV/√Hz)**	**S_{th} (nV/√Hz)**	**DR**
c-Si	113/6040	3.8	90	100	12.5	6.6	10.2	106
PolyA	96/4700	8.0	190	94	13.4	9.7	2.5	95

ACKNOWLEDGEMENTS

This work was supported by the European Research Council, Grant No. 240382 – DELPHINS project.

REFERENCES

[1] J. Arcamone, J. Philippe, G. Arndt, C. Dupre, M. Savoye, S. Hentz., T. Ernst, E Colinet, L. Duraffourg and E. Ollier "Nanosystems monolithically integrated with CMOS: emerging applications and technologies". *Proc. IEEE IEDM,* pp.: 22.1.1-22.1.4, Dec. 2014.

[2] J. L. Munoz-Gamarra, P. Alcaine, E. Marigo, J. Giner, A Uranga, J. Esteve and N. Barniol, "Integration of NEMS resonators in a 65 nm CMOS technology", *Microelec. Eng.,* vol. 110, pp. 246-249, Oct. 2013.

[3] D. Weinstein and S. A. Bhave, "The Resonant Body Transistor", *Nano Lett.*, vol. 10, pp. 1234–7, Feb. 2010.

[4] J. Philippe, G. Arndt, E. Colinet, M. Savoye, T. Ernst, E. Ollier and J. Arcamone, "Fully monolithic and ultra-compact NEMS-CMOS self-oscillator based-on single-crystal silicon resonators and low-cost CMOS circuitry", *IEEE International Conference on Micro Electro Mechanical Systems (MEMS)*, pp. 1071-4, Jan. 2014.

[5] S. Chong, B. Lee, K. B. Parizi, J. Provine, S. Mitra, R. T. Howe, and H.-S. P. Wong., "Integration of nanoelectromechanical (NEM) relays with silicon CMOS with functional CMOS-NEM circuit", *Electron Devices Meeting (IEDM)*, pp. 30-5, Dec. 2011.

[6] P. Batude, T. Ernst, J. Arcamone, G. Arndt, P. Coudrain, and P.-E. Gaillardonet, "Integration of Nanoelectromechanical (NEM) Relays with Silicon CMOS with Functional CMOS-NEM Circuit", *Journal on Emerging and Selected Topics in Circuits and Systems*, vol. 2, Dec. 2012.

[7] J. S. Im, H. J. Kim and M. O. Thompson, "Phase transformation mechanisms involved in excimer laser crystallization of amorphous silicon films", *Appl. Phys. Lett.*, vol. 63, 1969 Jul. 1993.

[8] E Mile, G Jourdan, I Bargatin, S Labarthe, CMarcoux, P Andreucci, S Hentz, C Kharrat, E Colinet and L Duraffourg, "In-plane nanoelectromechanical resonators based on silicon nanowire piezoresistive detection", *Nanotechnology,* vol. 21 165504 Mar. 2010.

[9] I. Bargatin, E. B. Myers, J. Arlett, B. Gudlewski and M. L. Roukes, "Sensitive detection of nanomechanical motion using piezoresistive signal downmixing", *App. Phy. Lett.*, vol. 86, 13, Mar. 2005.

CONTACT

Thomas Ernst, Thomas.ernst@cea.fr